
The repulsive Casimir force

Maikel van Putten, *Rijksuniversiteit Groningen*

August 31, 2015

This paper will look into research that has been done on the repulsive Casimir force using various methods to achieve this goal, such as metamaterials, geometry of the system or usage of an intervening liquid medium. This research will be critically reviewed and various applications will be shown for nano- and microelectromechanical systems. Repulsive Casimir force can be promising to prevent stiction and/or adhesion in NEMS/MEMS and can bring up new applications. A large amount of theoretical research has been done and numerical methods have shown big improvements in accuracy of calculations of the Casimir force for complicated systems. However, experimental research lags behind because of difficulties to measure these low forces and fabricating the complicated systems that have been proposed based on theoretical considerations.

Contents

1	Introduction	3
2	Theory	3
2.1	The Casimir effect	3
2.2	Lifshitz theory	5
2.3	Computational methods	6
2.4	Influence of surface roughness on the Casimir force	7
3	Changing the sign of the Casimir force	8
3.1	Casimir repulsion based on geometry	9
3.2	Casimir repulsion based on an intervening liquid medium	10
3.3	Casimir repulsion using metamaterials	11
3.4	Casimir repulsion in topological insulators	12
3.5	Lack of experimental proof	13
4	The Casimir force in nano-and microelectromechanical systems (NEMS and MEMS)	13
4.1	Graphene and the Casimir force	16
5	Conclusion	16
5.1	Outlook	17
6	Acknowledgements	17
7	References	17

1 Introduction

“I mentioned my results to Niels Bohr, during a walk. That is nice, he said, that is something new... and he mumbled something about zero-point energy.”

Hendrik Casimir

Hendrik B.G. Casimir and Dirk Polder showed in 1948 that the so-called London-van der Waals force behaves differently under larger distances [1]. As was calculated by Hamaker, Verwey and Overbeek, the London-van der Waals interaction energy between a colloidal particle and a perfectly conducting plate is proportional to r^{-3} and proportional to r^{-6} between two colloidal particles [2]. However for larger distances, a different distance dependence of this interaction energy was found, because of retardation of the London-van der Waals forces. It was found to be proportional to r^{-4} between a particle and a perfectly conducting plate and proportional to r^{-7} between two particles in the limit of large distances. Casimir found that the expressions for the interaction energy could also be found from the electromagnetic zero point energy and calculated it for two perfectly conducting parallel plates [3]. Later, E.M. Lifshitz and his colleagues came up with a general theory, combining both the Van der Waals force and the Casimir force for real materials by using the fluctuation-dissipation theorem [4].

In the last 20 years, the Casimir force showed increasing interest. Lamoureux did the first actual measurement of the Casimir force in 1997 [5] and a considerable amount of work on theoretical and experimental research has been done since then. An interesting aspect of the Casimir force, is the possibility for it to become repulsive under certain conditions, which was one of the conclusions of the work done by Lifshitz [4]. This can be promising for nano-and microelectromechanical systems (NEMS/MEMS), as stiction and adhesion are problematic, since the Casimir force is relatively large at this length scale [6]. The Casimir force might also be used to our benefit in certain systems [7]. This paper will look into the work that has been done on the repulsive Casimir force and its applications in NEMS and MEMS and will critically evaluate this research and show an outlook on the field of repulsive Casimir force and its applications.

2 Theory

2.1 The Casimir effect

To calculate the Casimir force, we consider two perfectly conducting plates in free space, both perpendicular to the z-axis separated by a distance a . The vibrations from the zero point electromagnetic field are then continuous along the x and y-axis and quantized along the z-axis, $k_z = \pm \frac{n\pi}{a}$. The vacuum energy of the electromagnetic field then is

$$\frac{1}{2} \sum \hbar\omega = \frac{\hbar c A}{2} \int_{-\infty}^{+\infty} \int_{-\infty}^{+\infty} \frac{dk_x dk_y}{(2\pi)^2} \sum_{n=-\infty}^{\infty} \sqrt{k_x^2 + k_y^2 + \left(\frac{n\pi}{a}\right)^2} \quad (1)$$

where A is the area of the plates. By using polar coordinates, $x = \sqrt{k_x^2 + k_y^2}$, and rearranging the sum we get

$$\frac{1}{2} \sum \hbar\omega = \frac{\hbar c A}{2} \int_0^{\infty} \frac{x dx}{\pi} \left(\sum_{n=0}^{\infty} \sqrt{x^2 + \left(\frac{n\pi}{a}\right)^2} - \frac{x}{2} \right) \quad (2)$$

where the last term is to correct for double counting of $n=0$. The next step is to compare this to the zero point energy without the plates. We can do this by assuming that a is very large, such that k_z becomes continuous as well.

$$\frac{E}{A} = \frac{\hbar c}{2} \int_0^\infty \frac{xdx}{\pi} \left(\sum_{n=0}^\infty \sqrt{x^2 + \left(\frac{n\pi}{a}\right)^2} - \frac{x}{2} - \frac{a}{\pi} \int_0^\infty dk_z \sqrt{x^2 + k_z^2} \right) \quad (3)$$

But this integral goes to infinity because of high k modes, a so-called ultraviolet divergence. One can neglect these high k modes because a real plate cannot reflect high frequency waves and therefore induce a cut-off for high k . There are different ways to regularize the function. Some of these methods are: heat kernel expansion, zeta function regularization, point splitting and frequency cut-off [8]. One important requirement should be that the final result is independent of the regularization method. Here we use a frequency cut-off function and use the Abel-Plana formula as used in reference [8]. First, by introducing a new variable, $t = ak_z/\pi$, we get

$$\frac{E}{A} = \frac{\hbar c}{2a} \int_0^\infty x dx \left(\sum_{n=0}^\infty \sqrt{\left(\frac{xa}{\pi}\right)^2 + n^2} - \frac{ax}{2\pi} - \int_0^\infty dt \sqrt{\left(\frac{xa}{\pi}\right)^2 + t^2} \right) \quad (4)$$

Now using the Abel-Plana formula

$$\sum_{n=0}^\infty F(n) - \int_0^\infty F(t) dt = \frac{1}{2} F(0) + i \int_0^\infty \frac{dt}{e^{2\pi t} - 1} [F(it) - F(-it)] \quad (5)$$

we get the following,

$$\frac{E}{A} = -\frac{\hbar c}{a} \int_0^\infty x dx \int_{\frac{xa}{\pi}}^\infty \frac{\sqrt{t^2 - \left(\frac{xa}{\pi}\right)^2}}{e^{2\pi t} - 1} dt \quad (6)$$

Which can be further simplified, by using $y = \frac{xa}{\pi}$ and changing the order of integration,

$$E = -\frac{\pi^2 \hbar c}{a^3} \int_0^\infty \frac{dt}{e^{2\pi t} - 1} \int_0^t y \sqrt{t^2 - y^2} dy = -\frac{\pi^2 \hbar c}{3a^3} \int_0^\infty \frac{t^3 dt}{e^{2\pi t} - 1} = -\frac{\pi^2 \hbar c}{720a^3} \quad (7)$$

As we can see, the result is independent of the regularization method that was used. Finally, the force per unit area is

$$P = -\frac{dE}{da} = -\hbar c \frac{\pi^2}{240a^4} \quad (8)$$

where a is the distance between the plates.

The Casimir effect is often being used as an argument for the zero point fluctuations of the vacuum, for instance in the discussion on dark energy. However, there is an enormous quantitative discrepancy between the theoretical value of the zero point energy of the electric field, 10^{95}g/cm^3 , and the actual dark energy in the universe, 10^{-29}g/cm^3 [9]. This theory has been refuted, since the Casimir force can also be computed without using zero-point energies as being a relativistic, quantum force between charges and current [10].

2.2 Lifshitz theory

“His calculations were so cumbersome that they were not even reproduced in the relevant Landau and Lifshitz volume, where, as a rule, all important calculations are given.”

Vitaly L. Ginzburg, 1979

After the work done by Casimir, Lifshitz extended his theory to real materials and unified the van der Waals force and the Casimir force [4]. He also studied the effect of temperature on the interaction between bodies. The theory was further generalized by Dzyaloshinskii in 1961 [11]. The Lifshitz theory takes the fluctuating electromagnetic field, as a starting point for the interaction between different bodies.

The fluctuating electromagnetic field can be obtained by using the fluctuation dissipation theorem. The fluctuation dissipation theorem gives the following result for currents,

$$\langle J_\alpha(\omega, \mathbf{r})(J_\beta^*(\omega', \mathbf{r}')) \rangle = \omega \epsilon''(\omega) \left(\frac{\hbar\omega}{2} + \frac{\hbar\omega}{e^{\hbar\omega/kT} - 1} \right) \delta(\omega - \omega') \delta(\mathbf{r} - \mathbf{r}') \delta_{\alpha\beta} \quad (9)$$

where $\epsilon''(\omega)$ is the imaginary part of the dielectric function of the material. Note that this equation does not only take the vacuum fluctuations into account, but also thermal excitations. The current creates a field which can interact with the other body,

$$E_\alpha(\omega, \mathbf{r}) = \frac{i}{\omega} \int d\mathbf{r}' G_{\alpha\beta}(\omega, \mathbf{r}, \mathbf{r}') J_\beta(\omega, \mathbf{r}') \quad (10)$$

where $G_{\alpha\beta}(\omega, \mathbf{r}, \mathbf{r}')$ is the Green function. The fluctuation dissipation theorem gives the following results for fields,

$$\langle E_\alpha(\omega, \mathbf{r}) E_\beta^*(\omega', \mathbf{r}') \rangle = 2\pi\hbar \coth \left(\frac{\hbar\omega}{2kT} \right) \text{Im} G_{\alpha\beta}(\omega, \mathbf{r}, \mathbf{r}') \delta(\omega - \omega') \quad (11)$$

The fluctuations of the magnetic field can be obtained from equation 11 by using the Maxwell equations. Now we can find the Casimir force by using the Maxwell stress tensor,

$$\sigma_{\alpha\beta} = \frac{1}{4\pi} \left[\langle E_\alpha E_\beta \rangle + \langle H_\alpha H_\beta \rangle - \frac{1}{2} (\langle E^2 \rangle + \langle H^2 \rangle) \delta_{\alpha\beta} \right] \quad (12)$$

Then the Casimir force is given by σ_{zz} . Now the next step is to get the Green function from the Maxwell equations which can be done with the following formula,

$$\left[\delta_\alpha \delta_\gamma - \delta_{\alpha\gamma} \left(\nabla^2 + \frac{\omega^2}{c^2} \epsilon(\omega, \mathbf{r}) \right) \right] G_{\gamma\beta}(\omega, \mathbf{r}, \mathbf{r}') = 4\pi \frac{\omega^2}{c^2} \delta_{\alpha\beta} \delta(\mathbf{r} - \mathbf{r}') \quad (13)$$

So the dielectric properties of the material are implemented into the equation for the Casimir force via the Green function. The boundary conditions for this equation is that the tangential components should be continuous. Equation 13 can be solved analytically for parallel plates, but requires numerical calculations for most geometries. For parallel plates, the force is given by the following formula,

$$F(d, T) = \frac{\hbar}{2\pi^2} \text{Re} \int_0^\infty d\omega \coth \frac{\hbar\omega}{2kT} \int_0^\infty dq q k_0 \sum_{v=s,p} \frac{r_1^v r_2^v e^{2ik_0 d}}{1 - r_1^v r_2^v e^{2ik_0 d}} \quad (14)$$

where r_j^v are the Fresnel coefficients and s and p stand for perpendicular and parallel polarizations, respectively,

$$r_j^s = \frac{k_0 - k_j}{k_0 + k_j}, \quad r_j^p = \frac{\epsilon_j k_0 - k_j}{\epsilon_j k_0 + k_j} \quad (15)$$

$$k_0 = i\sqrt{q^2 + \zeta^2/c^2}, \quad k_j = i\sqrt{q^2 + \epsilon(\zeta^2/c^2)}, \quad \epsilon_j = \epsilon_j(i\zeta) \quad (16)$$

Because equation 14 is both complex and oscillating over the real axis, it is easier to change to imaginary frequencies, giving the following representation for the force,

$$F(d, T) = \frac{kT}{\pi} \sum'_{n=0} \int_0^\infty dq q |k_0| \sum_{v=s,p} \frac{r_1^v r_2^v e^{-2|k_0|d}}{1 - r_1^v r_2^v e^{-2|k_0|d}} \quad (17)$$

where $\omega = i\zeta = \frac{2\pi kT}{\hbar} n$ and the prime above the summation indicates that the term for $n=0$ should be taken with a factor 1/2. equation 17 shows that a repulsive force is possible if

$$\frac{r_1^v r_2^v e^{-2|k_0|d}}{1 - r_1^v r_2^v e^{-2|k_0|d}} < 0 \quad (18)$$

which means that $r_1 r_2 < 0$ at imaginary frequencies. Using the Kramers-Kronig relation, we can relate $\epsilon(i\zeta)$ to the imaginary part of the dielectric function, which is proportional to the dissipation of the electromagnetic field,

$$\epsilon(i\zeta) = 1 + \frac{2}{\pi} \int_0^\infty d\omega \frac{\omega \epsilon''(\omega)}{\omega^2 + \zeta^2} \quad (19)$$

From the Lifshitz formula, the Van der Waals force and the Casimir force can be deduced as the non-retarded and retarded limit, respectively. Lifshitz theory is useful, because it is applicable for all distances and takes real optical properties of materials and temperature into account. However, it also has its limitations. The force can only be calculated analytically for parallel plates and sphere-plane geometries. Numerical calculation is necessary for other geometries. Also practical difficulties, like the surface roughness of a material, makes actual calculations difficult.

2.3 Computational methods

To solve problems regarding the Casimir force, both analytical and numerical approaches are still in use. To calculate new geometries, numerical methods are used most often. One of these methods is the proximity force approximation which can be used for nonplanar geometries. It is based on the Derjaguin approximation estimates forces between different geometries as forces between parallel plates [12, 13]. If the distance between two objects is much smaller than the typical curvature of the object, $d \ll R$, then the force can be approximated as the sum of the forces of small parallel plates which correspond to the shape of the object. For this reason, PFA should be used carefully and only in this limit [14]. The error of the proximity force approximation is of the order of d/R [15].

Another method was developed by Rodriquez et al. which is applicable for many geometries [16]. It uses a so-called finite-difference frequency domain (FDFD). The first step is to pick a contour or surface around the body of interest. Then for a certain frequency, equation 13 is solved for every grid point and

integrated to get the stress tensor (equation 12). Finally the stress tensor is integrated over all frequencies to obtain the force. This scheme does not require regularization and was found to have numerical convergence, which can be accelerated by subtracting the stress-tensor integral of the bodies over the integral of the isolated bodies [16]. Even though there might be numerical approaches that are more powerful for certain specific geometries, the FDFD approach is extremely useful because of its wide applicability.

Another method mentioned, is the boundary-element method (BEM). An advantage compared to FDFD is that only the boundaries of the bodies have to be discretized, and the unknowns on the surface are coupled to the Green's function of the homogeneous regions [16]. This method is efficient for problems where bodies are surrounded by infinite empty space. BEM discretizes the surface unknowns at the interface between different materials, which are coupled to one another by the Green's function.

Similar to FDFD, a finite-difference time domain (FDTD) method was developed by the same authors [17]. For the time domain approach, the Maxwell's equations are evolved in response to a delta-function current impulse, $\mathbf{J}(\mathbf{r}, t) = \delta(\mathbf{r} - \mathbf{r}')\delta(t - t')\hat{\mathbf{e}}_j$. The Green function can then be computed from the Fourier transform of the field,

$$G_{ij}^E(\xi; \mathbf{r}, \mathbf{r}') = -\frac{E_{ij}(\mathbf{r}, \xi)}{i\xi\mathcal{J}(\xi)} \quad (20)$$

where $\mathcal{J}(t) = \delta(t - t')$ and ξ is the frequency of the fields. Then the Casimir force can be obtained from the green function. Advantage of this FDTD is that it is possible to use already existing FDTD software to do the calculations. Another techniques that can be uses a so-called worldline approach, using Monte-Carlo techniques [18], but it is only considered for scalar fields and not for electromagnetic fields.

2.4 Influence of surface roughness on the Casimir force

An important correction on calculations and experiments is the surface roughness. The surface roughness can bring significant differences between theory and experiment [19]. Many surfaces, like evaporated metal films, have so-called self-affine roughness. Self-affinity is a name coming from fractal theory, where it refers to fractals where the pieces are scaled by different amounts in different directions. Self-affine roughness is characterized by the root mean squared roughness amplitude, the lateral correlation length (ξ) and the roughness exponent (H). These parameters can be found by doing AFM force measurements to determine the height difference correlation $H(r) = \langle |h(r) - h(0)|^2 \rangle$. For a self-affine surface

$$H(d) = \begin{cases} d^{2H} & d \ll \xi \\ 2w^2 & d \gg \xi \end{cases} \quad (21)$$

Most often perturbative PFA is used up to fourth order to correct the Casimir force for roughness effects [19]. This approach works if the RMS roughness is much smaller than the distance between the objects. These calculations use only the RMS roughness of the surface, while lateral parameters are also important for Casimir force measurements and should be corrected for if high surface slopes are apparent on the surface [19]. A second-order roughness correction based on numerical calculations has been given for two parallel metallic mirrors, taking the roughness correlation length and the RMS roughness amplitude into account [20].

The Casimir force between very rough surfaces where the peaks are much larger than the RMS and is comparable to the distance between the bodies, the Casimir force can be written as,

$$F_{Cas}(z) = F_{PT}(z) + F_{peaks}(z) \quad (22)$$

where $F_{PT}(z)$ is the Casimir force for rough surfaces which includes a contribution to flat surfaces and a perturbative roughness correction. $F_{peaks}(z)$ is the contribution to the Casimir force by the peaks, of which it is assumed that the contribution of the peaks is independent, because of the large distances between the peaks and can be taken into account using PFA [21]. It was found that roughness can influence the dynamics of MEMS at distances significantly larger than the RMS roughness, so it is something to bear in mind when considering NEMS/MEMS [22], which will be discussed in further detail in chapter 4.

3 Changing the sign of the Casimir force

Many parameters can be used in order to achieve repelling Casimir force. It can be done by using different geometries, immersing the bodies in a liquid, by using metamaterials and by using topological insulators (TIs). These different approaches will be shown in this chapter along with their (dis)advantages.

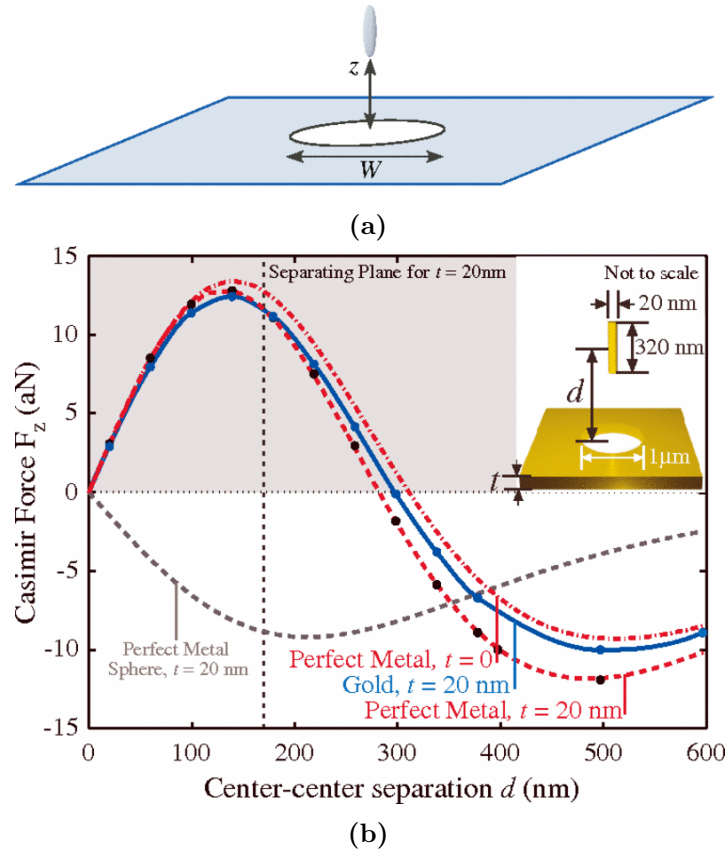


Figure 1: The top figure shows the schematic geometry that can achieve a repulsive Casimir force, an elongated metal particle above a metal plate with a hole. The bottom figure gives the Casimir force with respect to z (figure from [23]).

3.1 Casimir repulsion based on geometry

A system that has a repulsive Casimir force based on geometry has a few restrictions. As shown in reference [24], multilayer dielectric mirrors can't have repulsive Casimir force. Also for mirror-symmetric objects, the Casimir force can only be attractive [25]. An example of a system with repulsive Casimir force using a specific geometry is shown in figure 1 [23]. The ideal geometry in this case is an infinitesimal narrow needle which is only polarizable in the z direction above an infinitesimal thin plate with a hole (figure 1a). The explanation why there must be a repulsive Casimir force is rather simple and elegant:

Find a point \mathbf{x} such that the field of an oscillating electric dipole is unaffected by the presence of the metallic plate with a hole.

Then the Casimir energy is $U(\mathbf{x}) = U(\infty)$, which implies that the energy must vary non monotonically between \mathbf{x} and ∞ such that at some intermediate points, the Casimir force must be repulsive. In the case shown in figure 1a, when $\mathbf{x} = 0$, the field-lines of the dipole are perpendicular to the plate. So they are unaffected. Since for large z , the Casimir energy can be assumed to be unaffected by the hole, the Casimir force should be attractive. So there must be repulsive force for small z . Figure 1b shows the Casimir force for this geometry for a perfect metal and for gold, using BEM and FDTD. The repulsive Casimir force however can't lead to stable levitation. Based on Earnshaw's theorem stating that a collection of charges cannot be maintained in a stable equilibrium solely by electrostatic forces. This was further extended to fluctuation-induced forces resulting that Casimir forces are unstable if the permittivities of all object are higher or lower than that of the enveloping medium [26].

Another way to get a repulsive force between objects is by using the attractive Casimir force in a way that results in an overall repulsive force by using a specific geometry [27]. This was shown for a so-called Casimir "zipper" geometry, where metal brackets attached to two different substrates interlock (figure 2). The Casimir force between the metal brackets is attractive, but this leads to repulsion between the objects at a certain position (figure 3). Only numerical calculations

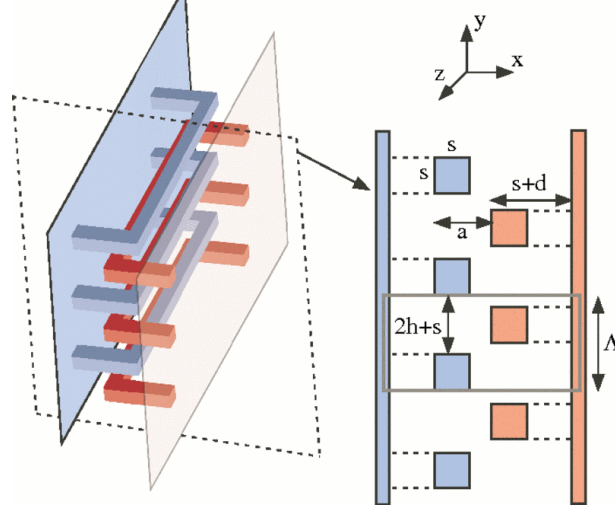


Figure 2: Schematic of the geometry of the Casimir zipper. The metal brackets interlock such that at a certain distance, the force between the brackets becomes attractive, resulting in a repulsive force between the complete object (figure from [27]).

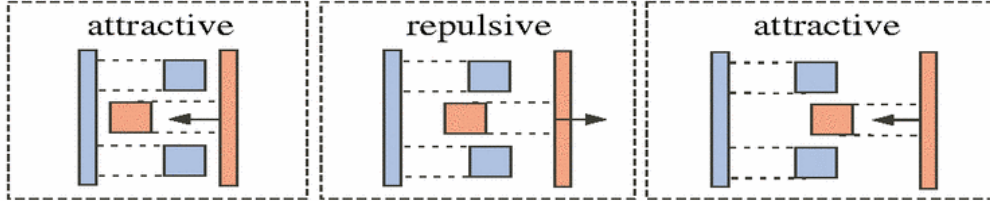


Figure 3: *If the brackets are interlocking and close to each other, the force between the objects is repulsive. However if the objects come close or move further apart, the net force is attractive (figure from [27]).*

were done for this system. Since it is solely based on geometry, the qualitative behaviour can be expected, but the quantitative behaviour also depends on surface roughness, imperfect metals and other deviations. As is often the case with research on the Casimir force, experimental research to confirm numerical calculations is lacking and is necessary to check the quantitative nature of this repulsive force. It is of course a great challenge to maintain a close parallel separation of these brackets [27].

3.2 Casimir repulsion based on an intervening liquid medium

Another approach is using a medium with its dielectric permittivity between the dielectric permittivity of the objects,

$$\epsilon_{object\ 1} < \epsilon_{medium} < \epsilon_{object\ 2} \quad (23)$$

Under these conditions, the requirements from equation 18 will be met and the force between object 1 and object 2 will be repulsive. One of the earliest known examples of this phenomenon is superfluidic helium in a container. The liquid helium will climb up the walls of the container, because the dielectric function of the liquid helium is between that of the container and the vapour [28]. This phenomenon is also shown in the retarded limit for a gold coated polystyrene sphere and a silica plate immersed in bromobenzene [29]. The sphere was attached to an AFM cantilever to measure the force. This was compared to the case of a

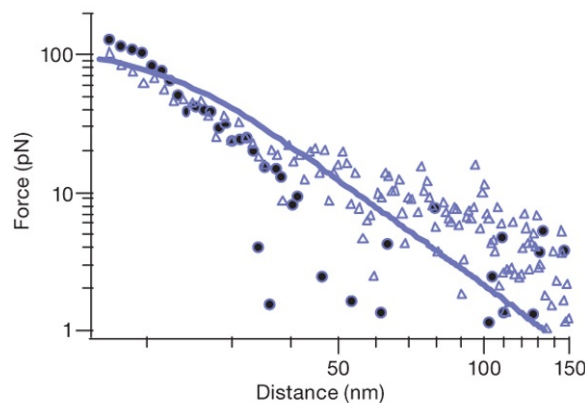


Figure 4: *Casimir force as a function of the distance between the sphere and the plate. The solid line indicates the calculated force using Lifshitz theory, including corrections for surface roughness. Triangles and circles are for different spheres with nominally the same diameter (figure from [29]).*

gold coated silica plate. In the case of a silica plate, the interaction is repulsive during both approach and retraction of the sphere. The force as a function of the distance is shown in figure 4 and shows agreement with Lifshitz theory.

3.3 Casimir repulsion using metamaterials

A third possible approach to achieve repulsive Casimir force is using metamaterials. Metamaterials are materials where the properties are engineered by changing the shape, geometry, size or orientation. This way the permittivity and permeability can be tuned, to get repulsive Casimir force. This idea was first shown by Timothy H. Boyer in 1974 [30]. It is shown that by using a left-handed metamaterials between two conducting plates, the sign of the force changes from attractive to repulsive [31]. The left-handed metamaterial functions as a perfect lens for metamaterials with $\epsilon(i\xi) = \mu(i\xi) = -1$ for frequencies $\xi < c/d$, where d is the distance between the two plates. Such left-handed metamaterials can be made of nanofabricated metal structures [32, 33, 34], and have shown to have some magnetic response in the visible range [35]. But this is extremely difficult. Magnetic dissipation leads to a decrease in the repulsive force. The magnetic permeability is low at near-infra red or optical frequencies (corresponding to the gaps on the order of micrometers that are typically measured [36]).

More detailed calculations on repulsion between two chiral metamaterials with more realistic frequency dependence were done and show that stable levitation is possible, but not for the metamaterials that they actually used to calculate this [37]. In later work by the same authors as reference [37], four different chiral metamaterial designs were checked on whether the chirality would be strong enough to achieve a repulsive Casimir force [38]. Figure 5 shows the structure of the four designs, Twisted-rosettes, Twisted-Crosswires, Four-U-SRRs and Conjugate-Swastikas, respectively. The chirality is maximized around the resonance frequency of the material, so the designs are modelled to work at a resonance frequency which in this case was taken to be 1 THz. They used a model where you can find the permittivity and permeability by doing reflection and transmission simulations on the design. The result of this paper is that the Four-U-SRRs and especially the Conjugate-Swastikas are the best option for metamaterials, because of the larger chirality that these structures have. However, the critical chirality required for repulsive Casimir force, was not yet reached by

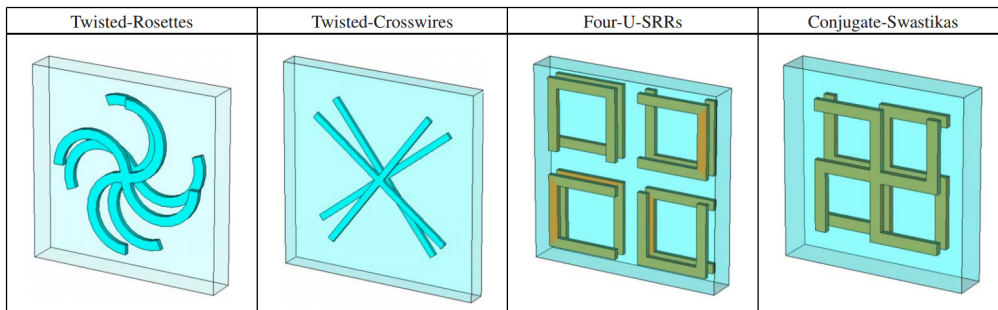


Figure 5: *Designs of the metamaterials that were tested to achieve repulsive Casimir force. From left to right, Twisted-Rosettes, Twisted-Crosswires, Four-U-SRRs, and Conjugate-Swastikas. The metamaterials consists of a slab of polyimide with two silver layers on top, embedded in polyimide. Each design has a different unit cell size to get the same frequency (figure from [38]).*

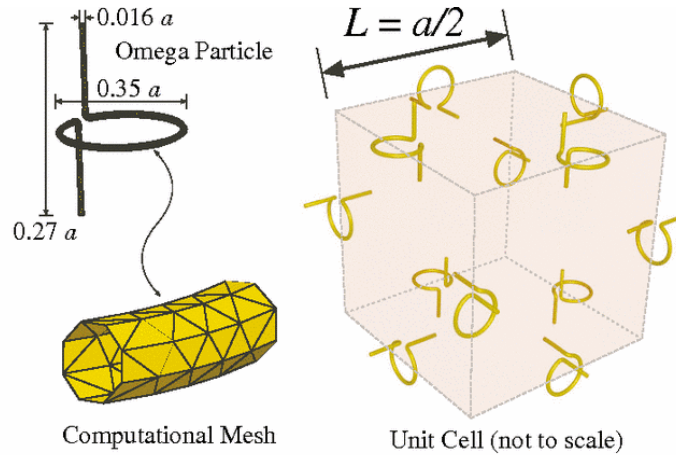


Figure 6: *The omega particles (shown left) will make up a unit cell as shown right. This gives an isotropic chiral material (figure from [39]).*

the designs in this paper.

The model that was used to calculate the repulsive Casimir force, assumes an isotropic media, however since the material is highly anisotropic, it is uncertain if this anisotropy will overwhelm the chirality of the material. Therefore, in reference [39] they do calculations using an isotropic chiral metamaterial. This metamaterial consists of so-called "omega" particles (figure 6). However, in the paper they conclude that to observe experimental proof, the measurements must be done with four digits of accuracy, where only 1% accuracy can be measured for simple geometries. Therefore they say that it is virtually impossible to detect the Casimir repulsive force for this metamaterial.

In contrast to the work done by Capasso [29] where a liquid was used as the medium, metamaterials can be used for completely frictionless MEMS/NEMS. More research on developing these metamaterials has to be done before it can be applied to experimentally examine repulsive Casimir forces and possible nanolevitation.

3.4 Casimir repulsion in topological insulators

Finally, a method was proposed to get a tunable Casimir force using Three-dimensional topological insulators (TIs) [40]. Topological insulators are exciting new materials, that were discovered only recently in 2007 for thin layers [41] and were shown for 3D materials in 2008 [42]. Topological insulators are materials with an insulating bulk, but with conducting surface states. The optical properties of such materials can then be used to get repulsive Casimir force, by adding a thin magnetic layer on top of the topological insulator, which makes the TI into a fully insulating material. The Casimir force can then be switched from attractive to repulsive by changing the sign of the magnetization on the surface and tuned by the distance between the two objects and by the sign of the topological magnetoelectric polarizability (TMEP). The TMEP allows to tune the optical properties of the materials. The Casimir energy density with respect to distance between the two TIs has a minimum, so repulsion exists for $d < d_m$ and there is attraction for $d > d_m$, where d_m is the distance of minimal Casimir energy density. Experimental research seems feasible, since the distance where the minimum

appears is $0.1 \mu\text{m}$ for TI BiSe₂. But there are challenges to get a high TMEP value to shift the minimum to the micrometer scale, which is difficult and requires full optical characterization of TIs to achieve this [40].

3.5 Lack of experimental proof

Even though the Casimir force is a field of high interest and intensive research [9], only a few papers can be found on experimental research on the repulsive Casimir force. One of the few papers that prove repulsive Casimir force is by Munday et al. [29]. The majority of the scientific papers are on theoretical research and numerical methods. There is a lot of debate on getting repulsive Casimir force by using a specific geometry or using metamaterials, but the only way to (dis)prove quantitative results is by doing experiments. The reason for this lack of experimental research is that it is highly complicated because of the weakness of the force and the complexity of methods that have been proposed. So it is important for the field of repulsive Casimir force that experimental research can catch up with the theoretical results that have been found in recent years, by trying to measure the weak Casimir forces and by fabricating complex structures like the zipper geometry [27] and the metamaterials [38].

4 The Casimir force in nano-and microelectromechanical systems (NEMS and MEMS)

A reason often mentioned to do research on the Casimir force is because of its effects in NEMS/MEMS. NEMS and to a lesser extent MEMS is an exciting new field where mechanical systems can potentially be used to measure quantum mechanical phenomena. Because of its strong distance dependence, the Casimir force can result in (unwanted) stiction or adhesion of parts in mechanical systems at small scale and is a common cause of NEMS/MEMS malfunction [6]. By achieving repulsive Casimir force in NEMS/MEMS, problem with stiction and adhesion can be resolved.

The attractive Casimir force can also be used to add new functionalities to NEMS/MEMS as has been shown in several papers [7, 43, 44, 45]. One of these examples is a micromachined torsional device (see figure 7) where the Casimir force causes an attraction between a plate, suspended on as substrate by two rods, and a sphere as they approach each other. This results in a torque in the plate, which can be detected by measuring the change in capacitance between the plate and the substrate [43].

Getting repulsive Casimir forces is not just a way to prevent stiction and adhesion but can also lead to frictionless NEMS/MEMS by levitation. One of the possible devices where the repulsive Casimir force can be used is for ultrasensitive force sensors and torque sensors [46]. An object can be immersed in a fluid above a surface where the conditions of equation 23 are met. The object will then levitate by counterbalancing gravity. The objects are then free to rotate or translate without static friction. Dynamic damping because of the viscosity of the fluid, will slow down the detection. An example of an application of this phenomenon is that one can put a ferromagnetic object to measure extremely weak external magnetic fields. However the choice of materials is limited because of the requirements for materials resulting from equation 23. An improvement would be if this levitation can be done without the immersion of the system in a

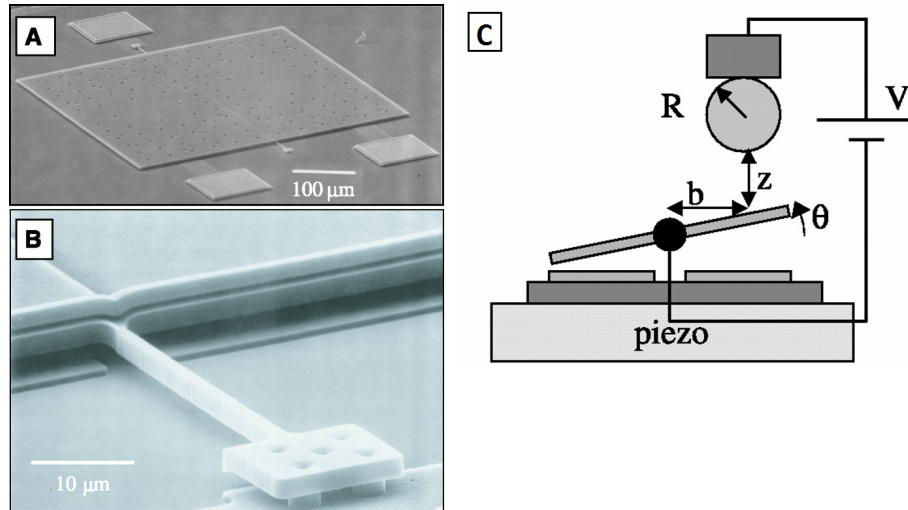


Figure 7: *A. a micromachined torsional device B. close up of the rods suspending the plate above the surface. The electrodes (small squares in figure A) connect to the top plate and to the left and right side of the substrate (figure from [43]).*

liquid, for instance by using metamaterials. Then dynamical damping is vanished, resulting in quick, precise measurements.

Repulsive Casimir force can also potentially be used for superlubricity [44]. Repulsive forces are well correlated with low friction, especially if this force increases for decreasing distance, improving to make sure the objects are separated. So a repulsive Casimir force results in low friction. They used a system with a thiolated gold particle and a flat PTFE substrate in anhydrous cyclohexane. They measured negative normal forces and a frictional force that was below the resolution of the instrument. For ethanol, where approximately zero force would be expected, the friction is still small but measurable.

Another micromechanical system that was proposed by using an intervening liquid to get repulsive Casimir force is torque measurements between two parallel birefringent slabs [7]. Birefringent materials have a refractive index that depends on the direction and polarization of the incident light. Often the refraction index in one direction, called the optic axis with refraction index n_e , is different with respect to all perpendicular directions with refraction index n_o . The quantum fluctuations between the two birefringent plates gives rise to a torque [47]. In reference [7], they propose an experiment with a small birefringent disk made out of quartz or calcite was placed parallel to a barium titanate plate in vacuum (see figure 8. The torque between the plates can then be measured if the plates are at submicrometer distance. But the plates will stick together at such distances because of the attractive Casimir force. However, the Casimir force can change sign by putting the system in a liquid, in this case ethanol was proposed. The disks floating on top of each other can then be used to measure the torque. For ethanol as intervening liquid, the force is repulsive at imaginary frequency below $\xi = 5 \cdot 10^{15}$ rad/s, corresponding to large distance, and attractive at higher imaginary frequencies, corresponding to short distances. So the disks should never be too close to each other to make sure that the Casimir force remains repulsive. By counterbalancing with gravity, the disk can levitate above the surface of the other disk.

Two important conditions for this to work are of course that the liquid should

not diminish the torque between the disks and that the disks can be brought close enough together while remaining levitation [7]. From their calculations, both conditions were met. Interestingly, the calculated torque between the two plates was actually higher when both plates were immersed in a liquid. The authors couldn't come up for an intuitive explanation of this phenomenon, but this would make it more feasible to measure the torque in the system with the liquid medium, as was proposed.

The disk can be rotated by shining on it with a laser beam, transferring angular momentum to the crystal. Once the laser beam is shut off, the disk should rotate back to the equilibrium position. Even though the authors mention in this paper, as well as other papers [48, 49, 50], that it should be feasible to proof this experimentally, such an experiment has not yet been carried out at the moment of writing this. This is again the common problem in Casimir research: the lack of experimental validation. There are some practical difficulties regarding such an experiment. The disks must be small (on the order of tens of microns in diameter) to avoid problems with parallelism between the two large surfaces. But smaller disks means a lower torque, so this requires more sensitive measurements. So there is a trade-off between keeping the disks parallel and having significant torque. Also surface roughness must be low, much smaller than $1\mu\text{m}$, and the area must be clean of dust [7]. Also it is possible that one detects other phenomena, like electrostatic effects or Brownian motion. However electrostatic effects can be screened easily by increasing the concentration of ions in the liquids [48] and Brownian motion can be statistically removed from the data by doing multiple runs [49].

Probably because of the difficulties to do such an experiment with birefringent disks, the same authors only recently proposed a new method to measure the torque [45]. In the article they propose an experiment where one of the birefringent crystals is replaced by an aligned liquid crystal, which will give a Casimir torque to the system. The liquid crystal is separated from the birefringent crystal by a thin, transparent layer of SiO_2 . If both crystals have positive birefringence, meaning that $\Delta n = n_e - n_o > 0$, then the liquid crystal will twist toward the extraordinary

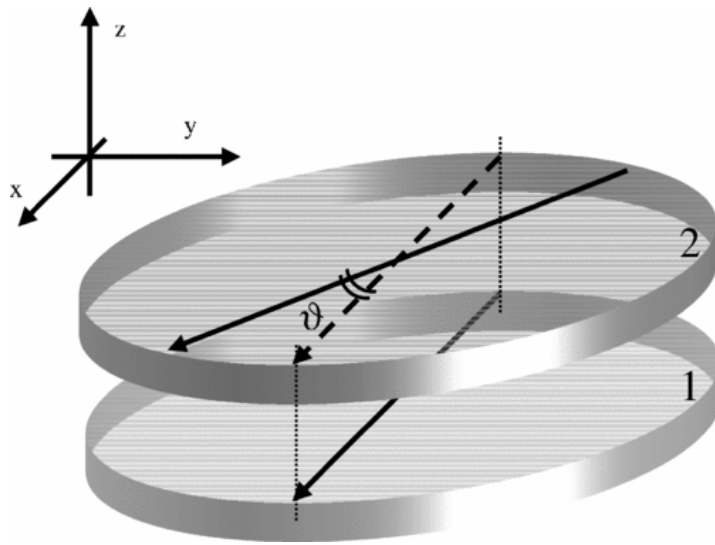


Figure 8: Two birefringent plates are placed parallel on top of each other. The optical axis is indicated by the arrow. The Casimir torque will make the plates turn until the optical axes of the two plates become parallel (figure from [7]).

axis of the solid crystal. They expect a measurable effect at separations of a few tens of nanometers. Advantage of such an experiment as to the one described before using two solid crystals, is that it is not necessary to levitate the disks in a liquid while at the same time keeping them parallel.

4.1 Graphene and the Casimir force

When studying the effect of the Casimir force on nano-and microelectromechanical systems, one cannot neglect graphene as a possible material. The Casimir force is also being studied regarding graphene and it raises the possibility to measure the Casimir force in truly two-dimensional structures [51, 52]. The dielectric properties are different for two-dimensional materials, could give new insights in the Casimir force. The force between two graphene sheets is calculated [51], assuming that graphene can be modelled as an infinitely, thin plasma sheet. The electrical conductivity of graphene is approximately constant ($\sigma_0 = e^2/4\hbar$), because of the energy band structure consisting of Dirac cones. The optical properties can be deduced from the electrical conductivity and the final Casimir force per unit area which was found after some calculation was

$$P \approx \frac{3\hbar c}{16\pi^2 d^4} \frac{2\pi\sigma_0}{c} = \frac{3e^2}{32\pi d^4} \quad (24)$$

So the fundamental constants of the speed of light and Planck disappear, because of the specific value of the conductivity of graphene. The ratio between the Casimir force for perfect conductors and the Casimir force for graphene sheets as mentioned in the paper is approximately 0.00538 [51]. Of course a lower value can be expected, because of the transparency of the graphene sheets, resulting in its small conductivity. The distance dependence of graphene is the same as for perfectly conducting plates. Similar calculations have been done for systems with a graphene sheet and other materials. Measurements have been done confirming the calculations based on a constant conductivity because of the Dirac model that was used [52].

So graphene has an attractive Casimir force as could be expected. But repulsion may be possible if the graphene is put on a metal, with the other object being the metamaterial. However this is only possible if the dielectric response from the metal contributes significantly [53], in other words, if the graphene does not affect the metal-metamaterial system significantly which brings us back to the situation discussed before in chapter 3.3. A possibility might be to use graphene for an actual experiment to show repulsive Casimir force as was shown in figure 1. Of course this would not be a trivial experiment but graphene could be used as a thin conductive sheet.

5 Conclusion

The repulsive Casimir force shows promising applications in NEMS/MEMS. A lot of research has been done in finding the conditions to have repulsive Casimir force, theoretical models and numerical calculation. This shows that in certain circumstances repulsive Casimir force can be achieved using metamaterials, a specific geometrical configuration or an intervening medium. This brings limitations to the application in NEMS/MEMS of such ideas and preventing stiction of micromechanical parts in systems. Casimir force can also be used to our benefit to make NEMS/MEMS, for instance in the case of Casimir torque

between two birefringent plates. To bring research on the Casimir force to the next level, experimental verification of theoretical results will be necessary. If this can be done in the future, full understanding of the Casimir force will get closer within our reach.

5.1 Outlook

It is fascinating to see that even 60 years after the discovery by of the Casimir force by Casimir and Polder, there is still a lot of research going on in this field. Especially as technology is scaling down and we go in to the regime where the Casimir force becomes more significant, the interest in research on the Casimir force increases. Many of the papers in the field are based on theoretical calculation on systems. Big improvements have been done on this aspect, with improving computational power and brute-force numerical approaches being developed [17, 54]. So in the future it can be expected that calculations can be done for more complex systems. What is often lacking is experimental verification. Experimental researchers are not yet capable of measuring the Casimir force for more complicated systems. Only few experiments have been done, for only simple systems, such as the sphere-plate configuration. In the case of metamaterials, a lot of work can still be done on fabrication and characterization of these materials, before it can be applied in experiment to get a repulsive Casimir force. To check theoretical calculations it is important that experiments in the future can verify the theoretical results.

Experimental research on the Casimir force gives many complications, for instance the weakness of the force and the size at which these measurements must be done. However it should be possible to do this kind of research in the future with improving fabrication techniques to fabricate devices and improvement of machines to characterize the devices and measure the Casimir force. This experimental research can be very useful for NEMS/MEMS, where stiction/adhesion becomes increasingly important at small scales.

6 Acknowledgements

I would like to thank the Zernike institute for receiving the fellowship, making it possible to fully commit to the Nanoscience programme. Also, I would like thank Prof. Dr. George Palasantzas for useful discussions and feedback on this research paper.

7 References

- [1] H. Casimir and D. Polder, "The influence of retardation on the london-van der waals forces," *Physical Review*, vol. 73, no. 4, p. 360, 1948.
- [2] E. Verwey, "Theory of the stability of lyophobic colloids.," *The Journal of physical chemistry*, vol. 51, no. 3, pp. 631–636, 1947.
- [3] H. B. Casimir, "On the attraction between two perfectly conducting plates," in *Proc. K. Ned. Akad. Wet*, vol. 51, p. 150, 1948.
- [4] E. Lifshitz, "The theory of molecular attractive forces between solids," 1956.
- [5] S. K. Lamoreaux, "Demonstration of the casimir force in the 0.6 to 6 m range," *Physical Review Letters*, vol. 78, no. 1, p. 5, 1997.

- [6] E. Buks and M. Roukes, “Stiction, adhesion energy, and the casimir effect in micromechanical systems,” *Physical Review B*, vol. 63, no. 3, p. 033402, 2001.
- [7] J. N. Munday, D. Iannuzzi, Y. Barash, and F. Capasso, “Torque on birefringent plates induced by quantum fluctuations,” *Physical Review A*, vol. 71, no. 4, p. 042102, 2005.
- [8] M. Bordag, G. L. Klimchitskaya, U. Mohideen, and V. M. Mostepanenko, *Advances in the Casimir effect*, p. Ch.4. Oxford University Press, 2009.
- [9] S. K. Lamoreaux, “Casimir forces: Still surprising after 60 years,” *Phys. Today*, vol. 60, no. 2, pp. 40–45, 2007.
- [10] R. Jaffe, “Casimir effect and the quantum vacuum,” *Physical Review D*, vol. 72, no. 2, p. 021301, 2005.
- [11] I. E. Dzyaloshinskii, E. Lifshitz, and L. P. Pitaevskii, “General theory of van der waals’ forces,” *Physics-Uspokhi*, vol. 4, no. 2, pp. 153–176, 1961.
- [12] B. V. Derjaguin, “Untersuchungen ber die reibung und adhsion, iv,” *Colloid Polymer Science*, vol. 69, no. 2, pp. 155–164, 1934.
- [13] J. Bocki, J. Randrup, W. wiatecki, and C. Tsang, “Proximity forces,” *Annals of Physics*, vol. 105, no. 2, pp. 427–462, 1977.
- [14] H. Gies and K. Klingmller, “Casimir effect for curved geometries: Proximity-force-approximation validity limits,” *Physical Review Letters*, vol. 96, no. 22, p. 220401, 2006.
- [15] M. Bordag, U. Mohideen, and V. M. Mostepanenko, “New developments in the casimir effect,” *Physics reports*, vol. 353, no. 1, pp. 1–205, 2001.
- [16] A. Rodriguez, M. Ibanescu, D. Iannuzzi, J. Joannopoulos, and S. G. Johnson, “Virtual photons in imaginary time: Computing exact casimir forces via standard numerical electromagnetism techniques,” *Physical Review A*, vol. 76, no. 3, p. 032106, 2007.
- [17] A. W. Rodriguez, A. P. McCauley, J. D. Joannopoulos, and S. G. Johnson, “Casimir forces in the time domain: Theory,” *Physical Review A*, vol. 80, no. 1, p. 012115, 2009.
- [18] H. Gies, K. Langfeld, and L. Moyaerts, “Casimir effect on the worldline,” *Journal of High Energy Physics*, vol. 2003, no. 06, p. 018, 2003.
- [19] P. V. Zwol, G. Palasantzas, and J. T. M. De Hosson, “Roughness corrections to the casimir force: The importance of local surface slope,” *Applied Physics Letters*, vol. 91, no. 14, p. 144108, 2007.
- [20] P. A. M. Neto, A. Lambrecht, and S. Reynaud, “Casimir effect with rough metallic mirrors,” *Physical Review A*, vol. 72, no. 1, p. 012115, 2005.
- [21] W. Broer, G. Palasantzas, J. Knoester, and V. B. Svetovoy, “Roughness correction to the casimir force beyond perturbation theory,” *EPL (Europhysics Letters)*, vol. 95, no. 3, p. 30001, 2011.
- [22] W. Broer, G. Palasantzas, J. Knoester, and V. B. Svetovoy, “Significance of the casimir force and surface roughness for actuation dynamics of mems,” *Physical Review B*, vol. 87, no. 12, p. 125413, 2013.
- [23] M. Levin, A. P. McCauley, A. W. Rodriguez, M. H. Reid, and S. G. Johnson, “Casimir repulsion between metallic objects in vacuum,” *Physical Review Letters*, vol. 105, no. 9, p. 090403, 2010.
- [24] A. Lambrecht, M.-T. Jaekel, and S. Reynaud, “The casimir force for passive mirrors,” *Physics Letters A*, vol. 225, no. 4, pp. 188–194, 1997.
- [25] O. Kenneth and I. Klich, “Opposites attract: A theorem about the casimir force,” *Physical Review Letters*, vol. 97, no. 16, p. 160401, 2006.

- [26] S. J. Rahi, M. Kardar, and T. Emig, “Constraints on stable equilibria with fluctuation-induced (casimir) forces,” *Physical Review Letters*, vol. 105, no. 7, p. 070404, 2010.
- [27] A. W. Rodriguez, J. D. Joannopoulos, and S. G. Johnson, “Repulsive and attractive casimir forces in a glide-symmetric geometry,” *Physical Review A*, vol. 77, no. 6, p. 062107, 2008.
- [28] E. Sabisky and C. Anderson, “Verification of the lifshitz theory of the van der waals potential using liquid-helium films,” *Physical Review A*, vol. 7, no. 2, p. 790, 1973.
- [29] J. N. Munday, F. Capasso, and V. A. Parsegian, “Measured long-range repulsive casimir-lifshitz forces,” *Nature*, vol. 457, no. 7226, pp. 170–173, 2009.
- [30] T. H. Boyer, “Van der waals forces and zero-point energy for dielectric and permeable materials,” *Physical Review A*, vol. 9, no. 5, p. 2078, 1974.
- [31] U. Leonhardt and T. G. Philbin, “Quantum levitation by left-handed metamaterials,” *New Journal of Physics*, vol. 9, no. 8, p. 254, 2007.
- [32] A. Grigorenko, A. Geim, H. Gleeson, Y. Zhang, A. Firsov, I. Khrushchev, and J. Petrovic, “Nanofabricated media with negative permeability at visible frequencies,” *Nature*, vol. 438, no. 7066, pp. 335–338, 2005.
- [33] S. Zhang, W. Fan, N. Panoiu, K. Malloy, R. Osgood, and S. Brueck, “Experimental demonstration of near-infrared negative-index metamaterials,” *Physical Review Letters*, vol. 95, no. 13, p. 137404, 2005.
- [34] V. M. Shalaev, W. Cai, U. K. Chettiar, H.-K. Yuan, A. K. Sarychev, V. P. Drachev, and A. V. Kildishev, “Negative index of refraction in optical metamaterials,” *Optics Letters*, vol. 30, no. 24, pp. 3356–3358, 2005.
- [35] V. M. Shalaev, “Optical negative-index metamaterials,” *Nature photonics*, vol. 1, no. 1, pp. 41–48, 2007.
- [36] F. Rosa, D. Dalvit, and P. Milonni, “Casimir-lifshitz theory and metamaterials,” *Physical Review Letters*, vol. 100, no. 18, p. 183602, 2008.
- [37] R. Zhao, J. Zhou, T. Koschny, E. Economou, and C. Soukoulis, “Repulsive casimir force in chiral metamaterials,” *Physical Review Letters*, vol. 103, no. 10, p. 103602, 2009.
- [38] R. Zhao, T. Koschny, E. Economou, and C. Soukoulis, “Comparison of chiral metamaterial designs for repulsive casimir force,” *Physical Review B*, vol. 81, no. 23, p. 235126, 2010.
- [39] A. P. McCauley, R. Zhao, M. H. Reid, A. W. Rodriguez, J. Zhou, F. Rosa, J. D. Joannopoulos, D. Dalvit, C. M. Soukoulis, and S. G. Johnson, “Microstructure effects for casimir forces in chiral metamaterials,” *Physical Review B*, vol. 82, no. 16, p. 165108, 2010.
- [40] A. G. Grushin and A. Cortijo, “Tunable casimir repulsion with three-dimensional topological insulators,” *Physical Review Letters*, vol. 106, no. 2, p. 020403, 2011.
- [41] M. Konig, S. Wiedmann, C. Brune, A. Roth, H. Buhmann, L. W. Molenkamp, X. L. Qi, and S. C. Zhang, “Quantum spin hall insulator state in hgte quantum wells,” *Science (New York, N.Y.)*, vol. 318, pp. 766–770, Nov 2 2007. JID: 0404511; CIN: Science. 2007 Nov 2;318(5851):758-9. PMID: 17975057; 2007/09/20 [aheadofprint]; ppublish.
- [42] D. Hsieh, D. Qian, L. Wray, Y. Xia, Y. S. Hor, R. Cava, and M. Z. Hasan, “A topological dirac insulator in a quantum spin hall phase,” *Nature*, vol. 452, no. 7190, pp. 970–974, 2008.

- [43] H. B. Chan, V. A. Aksyuk, R. N. Kleiman, D. J. Bishop, and F. Capasso, “Quantum mechanical actuation of microelectromechanical systems by the casimir force,” *Science (New York, N.Y.)*, vol. 291, pp. 1941–1944, Mar 9 2001. LR: 20070319; JID: 0404511; 2001/02/08 [aheadofprint]; ppublish.
- [44] A. A. Feiler, L. Bergstrm, and M. W. Rutland, “Superlubricity using repulsive van der waals forces,” *Langmuir*, vol. 24, no. 6, pp. 2274–2276, 2008.
- [45] D. A. Somers and J. N. Munday, “Rotation of a liquid crystal by the casimir torque,” *Physical Review A*, vol. 91, no. 3, p. 032520, 2015.
- [46] D. Iannuzzi, J. Munday, and F. Capasso *Ultra-low friction configuration*, 2005.
- [47] Y. S. Barash, “Moment of van der waals forces between anisotropic bodies,” *Radiophysics and Quantum Electronics*, vol. 21, no. 11, pp. 1138–1143, 1978.
- [48] F. Capasso, J. N. Munday, D. Iannuzzi, and H. Chan, “Casimir forces and quantum electrodynamical torques: Physics and nanomechanics,” *Selected Topics in Quantum Electronics, IEEE Journal of*, vol. 13, no. 2, pp. 400–414, 2007.
- [49] J. N. Munday, D. Iannuzzi, and F. Capasso, “Quantum electrodynamical torques in the presence of brownian motion,” *New Journal of Physics*, vol. 8, no. 10, p. 244, 2006.
- [50] D. Iannuzzi, M. Lisanti, J. N. Munday, and F. Capasso, “The design of long range quantum electrodynamical forces and torques between macroscopic bodies,” *Solid State Communications*, vol. 135, no. 9, pp. 618–626, 2005.
- [51] D. Drosdoff and L. M. Woods, “Casimir forces and graphene sheets,” *Physical Review B*, vol. 82, no. 15, p. 155459, 2010.
- [52] A. Banishev, H. Wen, J. Xu, R. Kawakami, G. Klimchitskaya, V. Mostepanenko, and U. Mohideen, “Measuring the casimir force gradient from graphene on a sio 2 substrate,” *Physical Review B*, vol. 87, no. 20, p. 205433, 2013.
- [53] D. Drosdoff and L. M. Woods, “Casimir interactions between graphene sheets and metamaterials,” *Physical Review A*, vol. 84, no. 6, p. 062501, 2011.
- [54] M. H. Reid, A. W. Rodriguez, J. White, and S. G. Johnson, “Efficient computation of casimir interactions between arbitrary 3d objects,” *Physical Review Letters*, vol. 103, no. 4, p. 040401, 2009.